International Journal of Advanced Trends in Computer Science and Engineering

Modeling and control a Robot serving a CNC Didactic Milling Machine

My Elhoussine ECH-CHHIBAT[1], Laidi ZAHIRI[2], Laila AIT EL MAALEM[3]
Laboratory of Signals, Intelligence Artificial and Systems Distributed, (SSDIA)
ENSET Mohammedia, Hassan II UniversityCasablanca, Morocco
[1]echchhibate@gmail.com, [2]zahirilaidi@yahoo.fr, [3]l.aitelmaalem@gmail.com

ABSTRACT

Robotics is a very dynamic field, which has been evolving diligently in these recent years. The pandemic disease hitting the world actually is accelerating significantly this development of robotics. The robot is a main factor that helps to ensure the distanciating in order to minimize the spread of this disease (Covid-19).Our contribution concerns mechanical production workshops, in this case, the automatic loading and unloading of a numerically controlled teaching machine, which implanted in our laboratory. The purpose is to reduce the manual manipulation of machine's parts and organs as much as possible, thus limiting the disease's spread by touch. In this work, we have developed all the models necessary to control the serial robot with six degrees of freedom. Three of those degrees control the position of the effector, and the three others orient the wrist. For this context, the direct and reversed geometric model, kinematic model and dynamic model were determined. A robot position and speed control methodology is proposed. Many simulations have been effectuated to properly validate the specific models sought

Key words: Robot, Kinematic,Torque, Dynamic, Control.

1. INTRODUCTION

At present, a large proportion of research work is oriented towards contributions that help to overcome this difficult phase that humanity is going through [1]. We are moving in this direction with a double objective. The first one is to help students to do their practical work with minimal man-machine contact. The second one is pedagogical so as to facilitate the learning and teaching of robotics based on validated models.

In order to conceive, simulate and control a robot, all the necessary data must be available, we mention the workspace in which the robot must operate and the different characteristics of the articulated structure. As mentioned above, several levels of modeling are also necessary, depending on the articulated structure of the system to be realized and the specifications of the charge notebook. However, the theoretical mathematical models are almost identical, but each one develops its own architecture, this is the biggest difficulty of robotics. Obtaining these different models is not simple; the difficulty varies according to the complexity of the kinematics of the articulated chain, the number of degrees of freedom, the type of joints and the nature of the structure (open, tree-like or closed). The initial parameterization is realized by using several methods. In our calculations, we use the modified Denavit-Hartenberg (DH) method [2] [3] [4].

2. MANIPULATOR DESIGN :

The served machine, Figure 1, is a machine driven by the standard graphic language. Its approximate dimensions are given in Table 1.

Figure 1:CNC machine tools

Table 1: Dimensions of the CNC milling machine

Height	width	depth
1.829m	1.067m	0.914m

The manipulator under study has three rotoid-type links, Figure 2. A pivot link with axis $z_1$and perpendicular to the other twoaxes ensures the vertical rotation of the manipulator between 0 and $\pi/2$. This movement covers the work area in front of the TORMACH PCNC 440 machine table. The other two swivel joints are parallel to each other and perpendicular to the first one, positioning the end point M of the manipulator in height. Note that in this specific robot, the second link is offset from the vertical axis by a length d_2 for a better arrangement of the workspace. The ball-and-socket connection of the gripper is ensured by three pivot connections with concurrent axes.
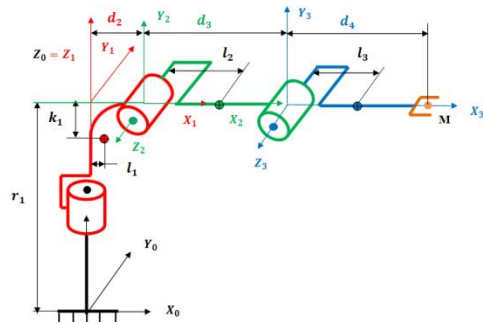
Figure 2: Kinematic structure of the manipulator

The dimensions of the manipulator are summarized in Table 2 and are expressed in meters.

Table 2: Dimensions of the manipulator

r_1	d_2	d_3	d_4
1.00 m	0.15m	0.80 m	0.80m

Environmental constraints force us to limit the robot's working field. The joint limits within which the manipulator operates are shown in Table 3.

Table 3: joint angular limits

θ_1	θ_2	θ_3
$0\ to\ \dfrac{\pi}{2}$	$0\ to\ \dfrac{\pi}{2}$	$0\ to\ -\dfrac{\pi}{2}$

2.1 Structure parameters (modified DH):

The passage from the reference R_{j-1} to the reference R_j is expressed as a function of four geometrical parameters [2] [5] [10]:

- α_j : Angle between axes z_{j-1} and z_j, corresponding to a rotation around x_{j-1} ;

- d_j : Distance between z_{j-1} and z_j along x_{j-1} ;
- θ_j : Angle between axes x_{j-1} et x_j, corresponding to a rotation around z_j ;
- r_j : Distance between axes x_{j-1} and x_j along z_j.

These elementary transformations are translated into simple translations or rotations:

$$Rot(x_{j-1}, \alpha_j), \ Tras(x_{j-1}, d_j), \ Rot(z_j, \theta_j) \ et \ Tras(z_j, d_j)$$

Table 4 summarizes the DH parameters of the robotic structure constituting the carrier.

Table 4: Structure parameters

	α_j	d_j	θ_j	r_i
$R_0 \longrightarrow R_1$	0	0	θ_1	r_1
$R_1 \longrightarrow R_2$	$+\dfrac{\pi}{2}$	d_2	θ_2	0
$R_2 \longrightarrow R_3$	0	d_3	θ_3	0

2.2 Trajectory planning

The control applied to the robot is determined by the architecture of the machine tool. The workpiece holder installed on the milling machine table is accessible from the main face of the machine Figure 1.

It is imperative that the robot clamp follows the path shown in Figure 3, and is carefully designed to avoid collisions and reduce unproductive time. The trajectory is composed of three different curves:

- Slightly upward engagement and disengagement to avoid friction with the table. This part concerns joints 2 and 3 ;
- A progressive rotation of the clamp, all three motors are involved;
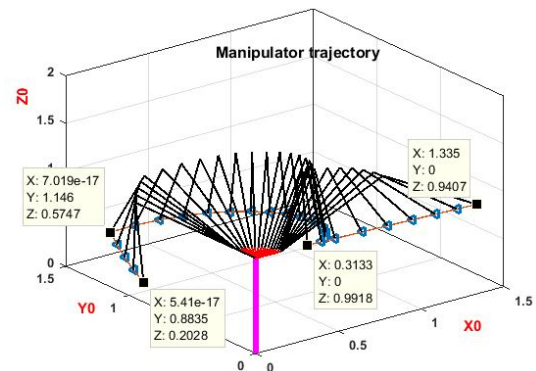- Gradual lowering of the gripper to deposit or pick up the workpiece.

Figure 3: Trajectory of manipulator gripper.

To move from one position to another, appropriate torques are applied to the joint motors. Position commands θ_{if} ($i = 1, 2, 3$) are applied to the system when it is in an initial position θ_{ji} ($j = 1, 2, 3$).

3. GEOMETRIC MODEL:

3.1 direct Model:

The homogeneous transformation matrix [8] [11] expresses the transition from a solid bound to the reference R_{j-1} to another solid bound to the reference R_j, the transition matrix is obtained by multiplying the elementary matrixes:

$$M_j^{j-1} = Rot(x_{j-1}, \alpha_j) * Tras(x_{j-1}, d_j) * Rot(z_j, \theta_j) * Tras(z_j, r_j) \quad (1)$$

The formula (1) is therefore:

$$M_j^{j-1} = \begin{pmatrix} cos(\theta_j) & -sin(\theta_j) & 0 & d_j \\ cos(\alpha_j) sin(\theta_j) & cos(\alpha_j) cos(\theta_j) & -sin(\alpha_j) & -r_j sin(\alpha_j) \\ sin(\alpha_j) sin(\theta_j) & sin(\alpha_j) cos(\theta_j) & cos(\alpha_j) & r_j cos(\alpha_j) \\ 0 & 0 & 0 & 1 \end{pmatrix}$$

For more space, we retain in the following symbolic writing:

$$c_i = cos(\theta_i) \ ; \ s_i = sin(\theta_i)$$
$$c_{ij} = cos(\theta_i + \theta_j) \ ; \ s_{ij} = sin(\theta_i + \theta_j)$$

120

The transformation matrices [7] between the robot segments considering the parameters in Table4are written as follows:

$$M_1^0 = \begin{pmatrix} c_1 & -s_1 & 0 & 0 \\ s_1 & c_1 & 0 & 0 \\ 0 & 0 & 1 & r_1 \\ 0 & 0 & 0 & 1 \end{pmatrix}; \quad M_2^1 = \begin{pmatrix} c_2 & -s_2 & 0 & d_2 \\ 0 & 0 & -1 & 0 \\ s_2 & c_2 & 0 & 0 \\ 0 & 0 & 0 & 1 \end{pmatrix}$$

$$M_3^2 = \begin{pmatrix} c_3 & -s_3 & 0 & d_3 \\ s_3 & c_3 & 0 & 0 \\ 0 & 0 & 1 & 0 \\ 0 & 0 & 0 & 1 \end{pmatrix}$$

Moving from the reference$R_3$to the reference$R_0$is obtained by the following matrix product:

$$M_3^0 = M_1^0 M_2^1 M_3^2 \qquad (2)$$

The global matrix$M_3^0$of the equation (2) can be written:

$$M_3^0 = \begin{pmatrix} c_1 c_2 c_3 - c_1 s_2 s_3 & -c_1 c_2 s_3 - c_1 s_2 c_3 s_1 & d_3 c_1 c_2 + d_2 c_1 \\ s_1 c_2 c_3 - s_1 s_2 s_3 & -s_1 c_2 s_3 - s_1 s_2 c_3 c_1 & d_3 s_1 c_2 + d_2 s_1 \\ s_2 c_3 + c_2 s_3 & -s_2 s_3 + c_2 c_3 & 0 & d_3 s_2 + r_1 \\ 0 & 0 & 0 & 1 \end{pmatrix}$$

Point M, Figure 2, has the following coordinates (d_4, 0, 0) in R_3. After calculation, its coordinates inR_0 are (3):

$$M \begin{pmatrix} c_1 c_{23} d_4 + d_3 c_1 c_2 + d_2 c_1 \\ s_1 c_{23} d_4 + d_3 s_1 c_2 + d_2 s_1 \\ s_{23} d_4 + d_3 s_2 + r_1 \\ 1 \end{pmatrix} (3)$$

3.2Inverse model:

The inverse problem [6], [9],[11] consists in evaluating the articular coordinates corresponding to a given position of the terminal organ, according to the Cartesian coordinates. The inverse geometrical model is used to calculate the position of each robot link as a function of the position and orientation of the end organ. The inverse matrix of the model is given as follows :

$$M_{j-1}^j = \begin{pmatrix} \cos(\theta_j) & \cos(\alpha_j)(\sin(\theta_j) & \sin(\alpha_j)\sin(\theta_j) & -d_j\cos(\theta_j) \\ -\sin(\theta_j) & \cos(\alpha_j)\cos(\theta_j) & \sin(\alpha_j)\cos(\theta_j) & d_j\sin(\theta_j) \\ 0 & -\sin(\alpha_j) & \cos(\alpha_j) & -r_j \\ 0 & 0 & 0 & 1 \end{pmatrix} (4)$$

(4) is used to write elementary inverse matrices :

$$M_0^1 = \begin{pmatrix} c_1 & s_1 & 0 & 0 \\ -s_1 & c_1 & 0 & 0 \\ 0 & 0 & 1 & -r_1 \\ 0 & 0 & 0 & 1 \end{pmatrix}; \quad M_1^2 = \begin{pmatrix} c_2 & 0 & s_2 & -d_2 c_2 \\ -s_2 & 0 & c_2 & d_2 s_2 \\ 0 & -1 & 0 & 0 \\ 0 & 0 & 0 & 1 \end{pmatrix};$$

$$M_2^3 = \begin{pmatrix} c_3 & s_3 & 0 & -d_3 c_3 \\ -s_3 & c_3 & 0 & d_3 s_3 \\ 0 & 0 & 1 & 0 \\ 0 & 0 & 0 & 1 \end{pmatrix}$$

The equations of the direct model are:

$$\begin{pmatrix} X_0 \\ Y_0 \\ Z_0 \\ 1 \end{pmatrix} = M_1^0 M_2^1 M_3^2 \begin{pmatrix} d_4 \\ 0 \\ 0 \\ 1 \end{pmatrix} (5)$$

To find the solutions to the inverse equation, the two members of equation (4) are premultiplied successively by the matricesM_{j-1}^jopposite of$M_j^{j-1}$for j varying from 1 to 3. These operations make it possible to isolate and identify the articular variablesθ_j we are looking for successively. In this case we proceed as follows:

By multiplying (5) on both sides byM_0^1 we get (6).

$$M_0^1 * \begin{pmatrix} X_0 \\ Y_0 \\ Z_0 \\ 1 \end{pmatrix} = M_2^1 * M_3^2 * \begin{pmatrix} d_4 \\ 0 \\ 0 \\ 1 \end{pmatrix} (6)$$

Once we do the math, we will have (7):

$$\begin{cases} X_0 c_1 + Y_0 s_1 = d_4(c_2 c_3 - s_2 s_3) + d_3 c_2 + d_2 \\ -X_0 s_1 + Y_0 c_1 = 0 \\ Z_0 - r_1 = d_4(s_2 c_3 + c_2 s_3) + d_3 s_2 \end{cases} (7)$$

The second line of (7) is an independent equation:

$$-X_0 s_1 + Y_0 c_1 = 0 (8)$$

We deduce θ_1 using the function atan2 [12]:

$$\theta_1 = atan2(Y_0/X_0)(9)$$

On either side, we multiply the relation (6) byM_1^2opposite of M_2^1, we get:

$$M_1^2 M_0^1 \begin{pmatrix} X_0 \\ Y_0 \\ Z_0 \\ 1 \end{pmatrix} = M_3^2 \begin{pmatrix} d_4 \\ 0 \\ 0 \\ 1 \end{pmatrix} (10)$$

After our calculation, we get (11):

$$\begin{cases} (X_0 c_1 + Y_0 s_1 - d_2)c_2 + (Z_0 - r_1)s_1 = d_4 c_3 + d_3 \\ (Z_0 - r_1)c_2 + (X_0 c_1 + Y_0 s_1 - d_2)s_2 = d_4 s_3 \end{cases} (11)$$

We put:

$$\begin{cases} A = (X_0 c_1 + Y_0 s_1 - d_2) \\ B = (Z_0 - r_1) \end{cases} (12)$$

So:

$$\begin{cases} Ac_2 + Bs_2 - d_3 = d_4 c_3 \\ Bc_2 - As_2 = d_4 s_3 \end{cases} (13)$$

By squaring, the two equations (13) to eliminate $\theta_3$and we get:

$$2Ad_3 c_2 + 2Bd_3 s_2 = A^2 + B^2 + d_3^2 - d_4^2 (14)$$

Equation (14) is written in the form:

$$K_1 s_2 + K_2 c_2 = K_3 \qquad (15)$$

With:$\begin{cases} K_1 = 2Bd_3 \\ K_2 = 2Ad_3 \\ K_3 = A^2 + B^2 + d_3^2 - d_4^2 \end{cases}$

Equation (15) is also written like the following:

$$(K_1^2 + K_2^2)s_2^2 - 2K_1 K_3 s_2 - (K_2^2 - K_3^2) = 0(16)$$

(16) is a second-order equation and its solutions are:

$$s_2 = \frac{K_1 K_3 \pm K_2 \sqrt{(K_1^2 + K_2^2 - K_3^2)}}{(K_1^2 + K_2^2)} (17)$$

$$c_2 = \frac{K_2 K_3 \pm K_1 \sqrt{(K_1^2 + K_2^2 - K_3^2)}}{(K_1^2 + K_2^2)} (18)$$

The relation between equations (17) and (18) makes possible to deduce θ_2 (19).

$$\theta_2 = atan2(s_2, c_2) (19)$$

θ_3(20) is evaluated by the relation of the two system equations (13):

$$\theta_3 = atan2(Bc_2 + As_2, \; Ac_2 + Bs_2 - d_3) \qquad (20)$$

The solution of the inverse geometric model is not unique; therefore, a point in robot space can be reached with several different postures. The choice of a posture is determined by the obstacles that exist in the workspace. Simulations are performed in MATLAB to validate the direct and inverse geometric models (Figure 4, 5, 6, and 7).

4. KINEMATIC MODEL

4.1 Direct kinematic model

The direct kinematic model expresses the speed of the end unit as a function of the joint speeds [7]. The direct model is calculated as follows (21):

$$\dot{X} = J(q)\dot{q} \qquad (21)$$

Where $J(q)$ denotes the Jacobian matrix of dimension (mxn) of the mechanism.

If for a configuration, $det(J(q)) = 0$, then there is a singularity. The robot gets instantly lost and the control program must react to these situations. The problem also arises if the robot is asked to reach points outside its working area (Figure 8, 9 and 10).

4.2 Inverse model:

The inverse kinematic model expresses the angular velocities of the joints as a function of wrist speed. The jacobian makes it possible to calculate a solution of the articular variables q knowing the operational coordinates X (22).

$$\dot{q} = J^{-1}(q)\dot{X} \qquad (22)$$

MATLAB scripts have been developed to validate the direct and inverse kinematic models of this manipulator.

4.3 Jacobian of the studied structure:

The Jacobian matrix is calculated by derivation of the direct geometric model:

$J_{ij} = \frac{\partial f_i}{\partial q_j}$ Where $i=1...m$ and $j=1...n$ and J_{ij} element (i, j) of the matrix $J(q)$.

From equation (3) the following Jacobian is deduced:

$$J(q) = \begin{pmatrix} -s_1(d_3 c_2 + d_4 c_{23} + d_2) & -c_1(d_3 * s_2 + d_4 s_{23}) & -d_4 c_1 s_{23} \\ c_1(d_3 c_2 + d_4 c_{23} + d_2) & -s_1(d_3 * s_2 + d_4 s_{23}) & -d_4 s_1 s_{23} \\ 0 & d_3 c_2 + d_4 c_{23} & d_4 c_{23} \end{pmatrix} (23)$$

5. DYNAMIC MODEL

5.1 Choice of model

The dynamic model is the relation between the static torsor (forces and torques) applied to the actuators of the links and the dynamic torsor of the robot segments. The dynamic model can be expressed by the relation (24), [13]:

$$\tau = f(q, \dot{q}, \ddot{q}, F_e) \qquad (24)$$

Where:

τ : Actuator torque/force vectors, depending on whether the joint is rotoid or prismatic.

q : Vector of joint positions.
$\dot{q}$: Articular velocity vector.
$\ddot{q}$: Vector of joint accelerations.

F_e: Vector representing the external forces (forces and torques) exerted by the manipulator on his environment.

Several formalisms are used to elaborate the dynamic equations of the robots. The best known formalisms are [14] :
- The formalism of Lagrange-Euler;
- The formalism of Newton-Euler.

In this work, we are interested in the formalism of Lagrange-Euler. The equations of this formalism [15] are:

$$\tau = \frac{d}{dt}\left(\frac{\partial L(q, \dot{q})}{\partial \dot{q}}\right) - \frac{\partial L(q, \dot{q})}{\partial q} \qquad (25)$$

Where the Lagrangian $L(q, \dot{q})$ is expressed as a function of the kinetic energy $E(q, \dot{q})$ and the potential energy $U(q)$ by relation [16]:

$$L(q, \dot{q}) = E(q, \dot{q}) - U(q) \qquad (26)$$

Equations (25) can be written as [16]:

$$\tau = D(q) * \ddot{q} + h(q, \dot{q}) + g(q) + b(\dot{q}) \qquad (27)$$

$D(q)$: Inertia matrix of dimension (n x n)
$h(q, \dot{q})$: Vector of centrifugal and Coriolis forces.
$g(q)$: Load gravity force vector.
$b(\dot{q})$: Friction in connections.

In this case, we study a didactic manipulator with three degrees of freedom of the rotoid type from which:

$$q = \begin{pmatrix} \theta_1 \\ \theta_2 \\ \theta_3 \end{pmatrix} \text{and} \tau = \begin{pmatrix} \tau_1 \\ \tau_2 \\ \tau_3 \end{pmatrix}$$

5.2Assessment of torques and forces

5.2.1Torques:

In the centre of each joint there is a torqueT_{ij}applied by arm i to arm j. The opposite torque is$T_{ij} = -T_{ji}$.The torques are expressed inR_0, they are respectively noted (28):

$$\begin{cases} T_{01} = (T_{01x}, T_{01y}, T_{01z}) \\ T_{12} = (T_{12x}, T_{12y}, T_{12z}) \\ T_{23} = (T_{23x}, T_{01y}, T_{23z}) \end{cases} \quad (28)$$

5.2.2 Forces applied to the manipulator arms

There are three forces of gravity applied to the centers of gravity of the robot segments, which are respectively namedG_i (i=1, 2, 3). If necessary, arm 3 can support a load of weight$G_L$at its end. These loads are expressed respectively by (29):

$$\begin{cases} G_i = -m_i g \\ G_L = -m_L g \end{cases} \quad (29)$$

Note that m_i is the mass of arm i, and m_L is the mass of the load.

5.2.3Generalized forces:

Generalized forces$\tau_i$are also expressed by (30) [17]:

$$\tau_i = \frac{\partial \omega}{\partial \dot{q}_\iota} T + \frac{\partial V_{ci}}{\partial \dot{q}_\iota} F \quad (30)$$

Where i=1, 2, 3.
Where ω is the angular velocity of the rigid body expressed in R_0, $V_{ci}$is the velocity of the center of mass of a solid in the base frameR_0.T and $F$are respectively the torque and the force acting on a segment of the robot.

In this case, the contribution to the generalized forceτ_i, of the different pivot links (1, 2, 3) is given respectively by (31):

$$\tau_i = \tau_{i1} + \tau_{i2} + \tau_{i3} \quad (31)$$

And:

$$\begin{cases} \tau_{i1} = \frac{\partial \omega_{10}}{\partial \dot{q}_\iota}(T_{01} - T_{12}) + \frac{\partial V_{G1}}{\partial \dot{q}_\iota} G_1 \\ \tau_{i2} = \frac{\partial \omega_{20}}{\partial \dot{q}_\iota}(T_{12} - T_{23}) + \frac{\partial V_{G2}}{\partial \dot{q}_\iota} G_2 \\ \tau_{i3} = \frac{\partial \omega_{30}}{\partial \dot{q}_\iota}(T_{23}) + \frac{\partial V_{G3}}{\partial \dot{q}_\iota} G_3 \end{cases} (32)$$

Therefore, the generalized forces$\tau_i$acting on the link are respectively expressed by:

$$\tau_1 = \frac{\partial \omega_{10}}{\partial \dot{q}_1}(T_{01} - T_{12}) + \frac{\partial V_{C1}}{\partial \dot{q}_1} G_1 + \frac{\partial \omega_{20}}{\partial \dot{q}_1}(T_{12} - T_{23}) + \frac{\partial V_{C2}}{\partial \dot{q}_1} G_2 + \frac{\partial \omega_{30}}{\partial \dot{q}_1}(T_{23}) + \frac{\partial V_{C3}}{\partial \dot{q}_1} G_3 + \frac{\partial V_M}{\partial \dot{q}_1} G_L \quad (33)$$

$$\tau_2 = \frac{\partial \omega_{10}}{\partial \dot{q}_2}(T_{01} - T_{12}) + \frac{\partial V_{C1}}{\partial \dot{q}_2} G_1 + \frac{\partial \omega_{20}}{\partial \dot{q}_2}(T_{12} - T_{23}) + \frac{\partial V_{C2}}{\partial \dot{q}_2} G_2 + \frac{\partial \omega_{30}}{\partial \dot{q}_2}(T_{23}) + \frac{\partial V_{C3}}{\partial \dot{q}_2} G_3 + \frac{\partial V_M}{\partial \dot{q}_2} G_L \quad (34)$$

$$\tau_3 = \frac{\partial \omega_{10}}{\partial \dot{q}_3}(T_{01} - T_{12}) + \frac{\partial V_{C1}}{\partial \dot{q}_3} G_1 + \frac{\partial \omega_{20}}{\partial \dot{q}_3}(T_{12} - T_{23}) + \frac{\partial V_{C2}}{\partial \dot{q}_3} G_2 + \frac{\partial \omega_{30}}{\partial \dot{q}_3}(T_{23}) + \frac{\partial V_{C3}}{\partial \dot{q}_3} G_3 + \frac{\partial V_M}{\partial \dot{q}_3} G_L \quad (35)$$

Calculations are giving (36):

$$\begin{cases} \tau_1 = T_{01z} \\ \tau_2 = T_{12z} - m_3 g L_3 c_{23} - m_2 g L_2 c_2 - m_3 g d_3 c_2 \\ \qquad - m_c g d_4 c_{23} - m_c g d_3 c_2 \\ \tau_3 = T_{23z} - m_3 g L_3 c_{23} - m_c g d_4 c_{23} \end{cases} (36)$$

5.3Lagrangian calculation of the articulated system

5.3.1Kinetic energy

The calculation of the kinetic energy of a body depends on its linear velocity, angular velocity and the moments of inertia of its components.

The inertia matrices of the manipulator segments are expressed at the centers of mass. Solids 2 and 3 are assumed to be symmetrical with respect to axes x_2 and x_3 respectively. Solid 1 is symmetrical with respect to the$x_1 z_1$plane. The inertia matrices are of the form:

$$I_1 = \begin{pmatrix} I_{x1} & 0 & -I_{x1z1} \\ 0 & I_{y1} & 0 \\ -I_{x1z1} & 0 & I_{z1} \end{pmatrix}; I_2 = \begin{pmatrix} I_{x2} & 0 & 0 \\ 0 & I_{y2} & 0 \\ 0 & 0 & I_{z2} \end{pmatrix}$$

$$I_3 = \begin{pmatrix} I_{x3} & 0 & 0 \\ 0 & I_{y3} & 0 \\ 0 & 0 & I_{z3} \end{pmatrix}$$

The kinetic energy of a body i is expressed byE_i (37):

$$\begin{cases} E_1 = \frac{1}{2}[\omega_{10} I_1 \omega_{10}^T + m_1 v_{G1}^2] \\ E_2 = \frac{1}{2}[\omega_{20} I_2 \omega_{20}^T + m_2 v_{G2}^2] \\ E_3 = \frac{1}{2}[\omega_{30} I_3 \omega_{30}^T + m_3 v_{G3}^2] \end{cases} \quad (37)$$

Where :

$$\begin{cases} \omega_{10} = (0,0,\dot{\theta}_1) \\ \omega_{20} = \omega_{10} + M_1^0 M_2^1 \omega_{22}^T \\ \omega_{30} = \omega_{20} + M_1^0 M_2^1 M_3^2 \omega_{33}^T \end{cases}$$

$\omega_{11} = (0,0,\dot{\theta}_1)$; $\omega_{22} = (0,0,\dot{\theta}_2)$; $\omega_{33} = (0,0,\dot{\theta}_3)$;
$\omega_{ii}$is the angular velocity of the solid i in the frame R_i;
$\omega_{i0}$is the angular velocity of the solid i in the frame R_0;
$\omega_{i0}^T$is the transpose of ω_{i0} ;
$v_{Gi}$is the linear velocity of the centre of mass of the solid i in the reference frame R_0.

The coordinates of the center of mass of segment 1 in the base frame $R_0$are:

$$\begin{cases} x_{01} = l_1 c_1 \\ y_{01} = l_1 s_1 \\ z_{01} = r_1 - k_1 \end{cases} (38)$$

The coordinates of the center of mass of segment 2 in the base frame $R_0$are:

$$\begin{cases} x_{02} = d_2 c_1 + l_2 c_1 c_2 \\ y_{02} = d_2 s_1 + l_2 s_1 c_2 \\ z_{02} = l_2 s_2 + r_1 \end{cases} (39)$$

The coordinates of the center of mass of segment 3 in base frame R_0 are:

$$\begin{cases} x_{03} = d_2 c_1 + l_3 c_1 c_{23} + d_3 c_1 c_2 \\ y_{03} = d_2 s_1 + l_3 s_1 c_{23} + d_3 s_1 c_2 \\ z_{03} = l_3 s_{23} + d_3 s_2 + r_1 \end{cases} (40)$$

By derivation of (38), (39) and (40), we obtain the speeds of the centers of gravity of arms 1, 2 and 3:

$$v_{G1} = \begin{cases} \dot{x_{01}} = -a\dot{\theta}_1 s_1 \\ \dot{y_{01}} = a\dot{\theta}_2 c_1 \\ \dot{z_{01}} = 0 \end{cases} (41)$$

And

$$v_{G2} = \begin{cases} \dot{x_{02}} = -d_2\dot{\theta}_1 s_1 - l_2[\dot{\theta}_1 s_1 c_2 + \dot{\theta}_2 c_1 s_2] \\ \dot{y_{02}} = d_2\dot{\theta}_1 c_1 + l_2[\dot{\theta}_1 c_1 c_2 - \dot{\theta}_2 s_1 s_2] \\ \dot{z_{02}} = l_2\dot{\theta}_2 c_2 \end{cases} (42)$$

And finally:

$$v_{G3} = \begin{cases} \dot{x_{03}} = -l_3[\dot{\theta}_1 s_1 c_{23} + (\dot{\theta}_2 + \dot{\theta}_3)c_1 s_{23}] - d_3[\dot{\theta}_1 s_1 c_2 + \dot{\theta}_2 c_1 s_2] - d_2\dot{\theta}_1 s_1 \\ \dot{y_{03}} = l_3[\dot{\theta}_1 c_1 c_{23} - (\dot{\theta}_2 + \dot{\theta}_3)s_1 s_{23}] + d_3[\dot{\theta}_1 c_1 c_2 - \dot{\theta}_2 s_1 s_2] - d_2\dot{\theta}_1 c_1 \\ \dot{z_{03}} = l_3(\dot{\theta}_2 + \dot{\theta}_3)c_{23} + d_3\dot{\theta}_2 c_2 \end{cases} (43)$$

In the end, the total kinetic energy is then:

$$E = E_1 + E_2 + E_3 \quad (44)$$

The final result is calculated by a Matlab script to avoid possible errors.

5.3.2 Calculation of the potential energy of the structure:

The total potential energy is given by the following relation:

$$U = m_1 g z_{01} + m_2 g z_{02} + m_3 g z_{03} \quad (45)$$

By calculating, we get:

$$U = g[m_1(r_1 - k_1) + m_2(r_1 + l_2 s_2) + m_3(r_1 + d_3 s_2 + l_3 s_{23})]$$

5.3.3 Dynamic structural equation:

The differential equations of the articulated system are expressed by the following relationships [17] [18].

$$\begin{cases} \tau_1 = \frac{d}{dt}\left(\frac{\partial L(\theta_1,\dot{\theta}_1)}{\partial\dot{\theta}_1}\right) - \frac{\partial L(\theta_1,\dot{\theta}_1)}{\partial\theta_1} \\ \tau_2 = \frac{d}{dt}\left(\frac{\partial L(\theta_2,\dot{\theta}_2)}{\partial\dot{\theta}_2}\right) - \frac{\partial L(\theta_2,\dot{\theta}_2)}{\partial\theta_2} \\ \tau_3 = \frac{d}{dt}\left(\frac{\partial L(\theta_3,\dot{\theta}_3)}{\partial\dot{\theta}_3}\right) - \frac{\partial L(\theta_3,\dot{\theta}_3)}{\partial\theta_3} \end{cases} (46)$$

By identification between equations (36) and (46), the torques at the joints are deduced, they are carried by the z_i axis of the i link. These are the equations of motion of the articulated structure. It is also the direct dynamic model (47).

$$\begin{cases} T_{01z} = \frac{d}{dt}\left(\frac{\partial L(\theta_1,\dot{\theta}_1)}{\partial\dot{\theta}_1}\right) - \frac{\partial L(\theta_1,\dot{\theta}_1)}{\partial\theta_1} \\ T_{12z} = \frac{d}{dt}\left(\frac{\partial L(\theta_2,\dot{\theta}_2)}{\partial\dot{\theta}_2}\right) - \frac{\partial L(\theta_2,\dot{\theta}_2)}{\partial\theta_2} + m_3 g L_3 c_{23} + m_2 g L_2 c_2 + \\ \quad m_3 g d_3 c_2 + m_L g d_4 c_{23} + m_L g d_3 c_2 \\ T_{23z} = \frac{d}{dt}\left(\frac{\partial L(\theta_3,\dot{\theta}_3)}{\partial\dot{\theta}_3}\right) - \frac{\partial L(\theta_3,\dot{\theta}_3)}{\partial\theta_3} + m_3 g L_3 c_{23} + m_L g d_4 c_{23} \end{cases} (47)$$

5.3.4 Proposed command:

Several control techniques are used in robotics [19], [20]. In this context, dynamic control is preferred. The system under study presents non-linear and strongly coupled dynamic equations. A gravity vector is brought into the control equations to overcome the above problems.

The PD control equations used are (48):

$$\begin{cases} T_{01z} = K_{s1}\frac{d(\theta_{1f}-\theta_1)}{dt} + K_{p1}(\theta_{1f} - \theta_1) \\ T_{12z} = K_{s2}\frac{d(\theta_{2f}-\theta_2)}{dt} + K_{p2}(\theta_{2f} - \theta_2) + m_3 g L_3 c_{23} + m_2 g L_2 c_2 + \\ \quad m_3 g d_3 c_2 + m_c g d_4 c_{23} + m_c g d_3 c_2 \\ T_{23z} = K_{s3}\frac{d(\theta_{3f}-\theta_3)}{dt} + K_{p3}(\theta_{3f} - \theta_3) + m_3 g L_3 c_{23} + m_c g d_4 c_{23} \end{cases} (48)$$

K_{pi} and K_{si} are respectively position and speed gains. θ_{if} is the desired angular position for joint i, Figure 3.

The identification between equations (47) and (48) gives us the results we are looking for. The differential equations are solved numerically using MATLAB scripts.

6. SIMULATIONS AND DISCUSSIONS:

6.1 Direct geometric model

It is validated by Figure 4 plotted for $\theta_1 = -\frac{\pi}{2}$ à $+\frac{\pi}{2}$, $\theta_2 = 0$ and $\theta_3 = 0$ and Figure 5 plotted for $\theta_1 = 0$, $\theta_2 = -\frac{\pi}{2}$ to $+\frac{\pi}{2}$ and $\theta_3 = 0$.
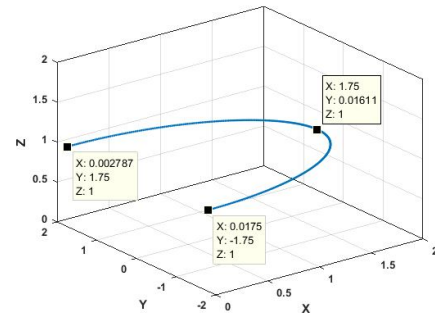

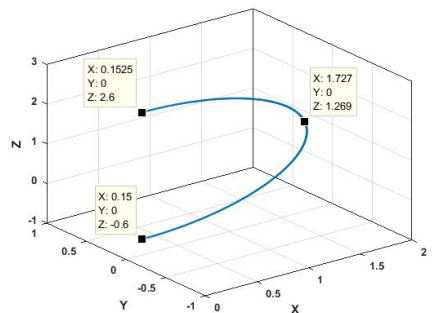**Figure 4:** Horizontal wrist space

Figure 5: Vertical wrist space

The overall working space of the manipulator in accordance with the technical specifications listed in Table 3 above, is shown in Figure 6.
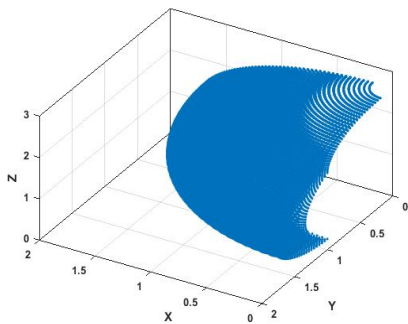
Figure 6: Robot workspace

6.2Inverse geometric model:

Simulations are performed on a case-specific graphical user interface designed in MATLAB. The interface is composed of three parts; the left part is reserved for the different postures. The right field is made up of two frames, the upper frame is designed for the direct model, in this part, we give the value of the angles and we recover the absolute cartesian coordinates X_0, Y_0 and Z_0. The lower frame checks the inverse geometric model, the cartesian coordinates are retrieved, and the system returns the angular coordinates. These results will be useful to check the position command of the system. Figure 7 clarifies this.
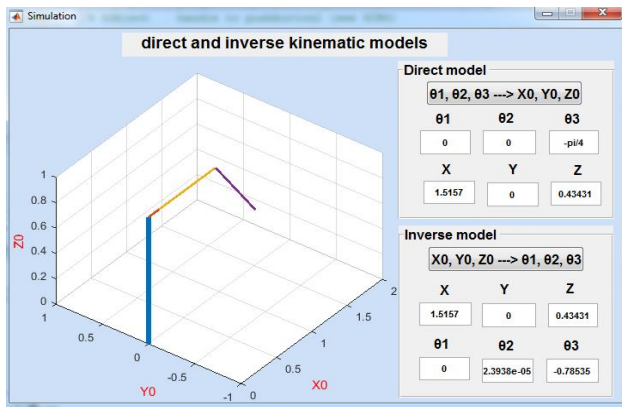
Figure 7:A position in space.

6.3Direct kinematic model

Note that the angular velocities are constant in all subsequent kinematic simulations.

Case 1:$\dot{\theta}_2 = \dot{\theta}_3 = 0and\dot{\theta}_1 = 0.1rd/s$.

In Figure 8, the plot corresponds to the linear velocity along the two axes X_0, Y_0 while the velocity V_Z is a zero.
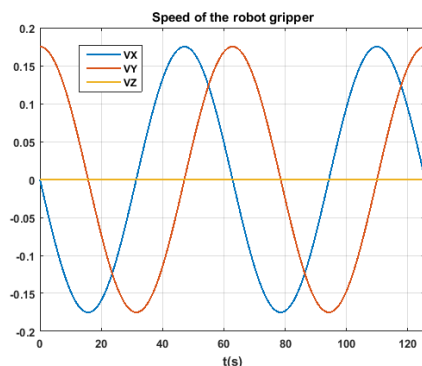

Figure 8: Wrist linear velocity case 1.

Case 2:$\dot{\theta}_1 = 0.1rd/s, \dot{\theta}_2 = 0.1rd/sand\dot{\theta}_3 = 0$

The wrist generates a trajectory around axes Z_1 and Z_2, the robot in this case has two degrees of freedom.The linear velocities V_X, V_Y and $V_Z$along the three axes, for this second case, are shown in Figure 9.
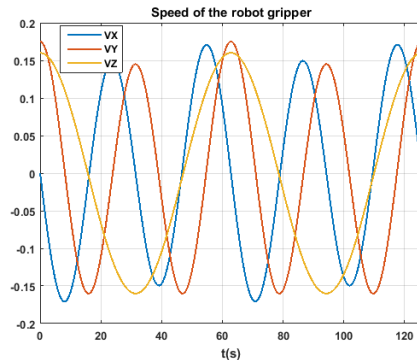

Figure 9: Wrist linear velocity case 1

Case 3: $\dot{\theta}_1 = \dot{\theta}_2 = \dot{\theta}_1 = 0.1rd/s$

The linear velocity of the robot end in any given case is explained in Figure 10.
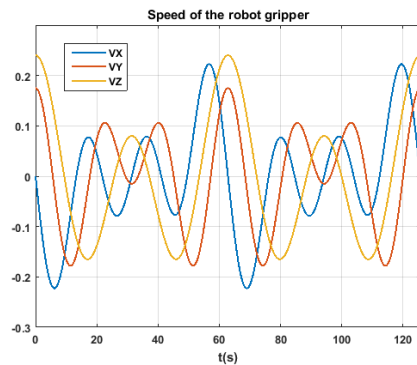

Figure 10: Speed per axis, case 3

6.4Dynamic model

Table 5 gives the indicative values of the parameters used to validate the dynamic control proposed above for this training robot:

Table 5: Indicative parameters values

I_{1z}	I_{2x}	I_{2y}	I_{2z}	I_{3x}	I_{3y}	I_{3z}	G
0.5	0.5	0.5	0.5	0.5	0.5	0.5	0.98
L_1	L_2	L_3	k_1	m_1	m_2	m_3	m_L
0.1	0.4	0.4	0.2	3	3	3	2

6.4.1System's step response:

The gripper is controlled to move from an initial position ($\theta_{1i} = 0, \theta_{2i} = 0$, $\theta_{3i} = 0$) to an end position ($\theta_{1f} = \frac{\pi}{2}$, $\theta_{2f} = \frac{\pi}{2}$, $\theta_{3f} = -\frac{\pi}{2}$). Figure 11 shows that the selected controller meets our needs very well. The correct setting of the coefficientsK_{si} andK_{pi}allows getting better results.
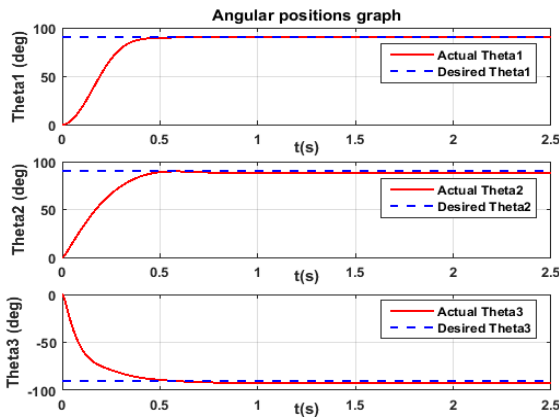
Figure 11: Angular position control

The motor speeds will be zero when the desired position is reached, Figure 12.
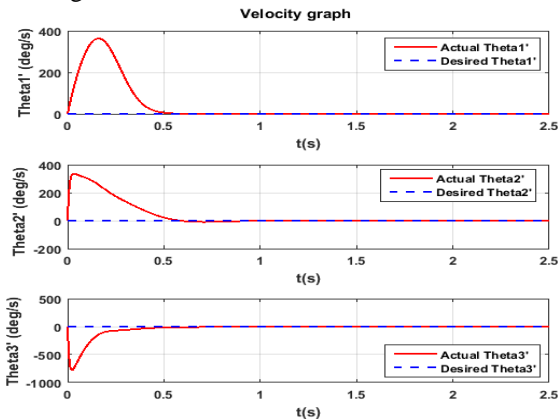

Figure 12 : Angular speed control

The motor torques acting on the robot segments to reach the desired position are shown in Figure 13. Note that torques T_2 and T_3 do not cancel each other even if the target is reached because of the weight of the components.
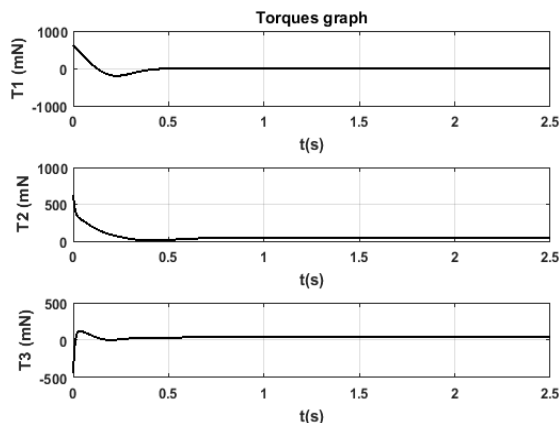

Figure 13 : Motor torques

6.4.2 System's sinus response:

In the following case the desired position is sinusoidal in the form$\theta_{if} = A_i \sin(\omega_i t)$, The initial conditions taken in the following simulations are $(\theta_{1i} = \frac{\pi}{8}, \theta_{2i} = \frac{\pi}{6}, \theta_{3i} = \frac{\pi}{4})$.

The signal reaches the desired destination very quickly, which justifies a good choice of model as well as position and speed gains. The convergence isquiteclear in Figures 14 and 15.
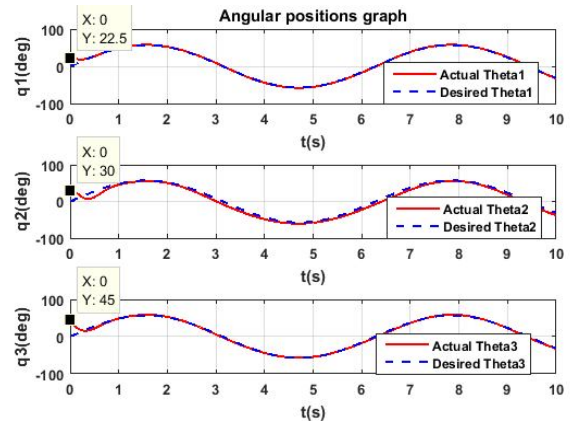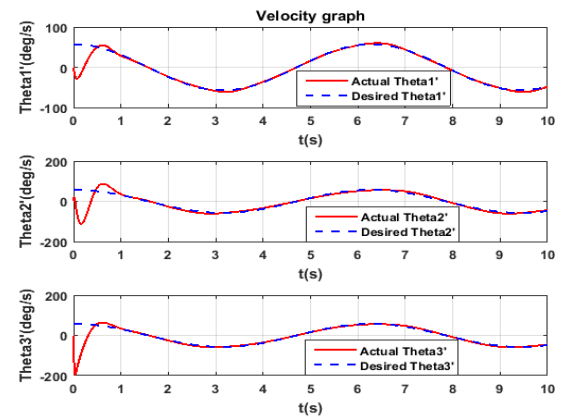

Figure 14: Sinusoidal signal control.

Figure 15 : Joint speed control

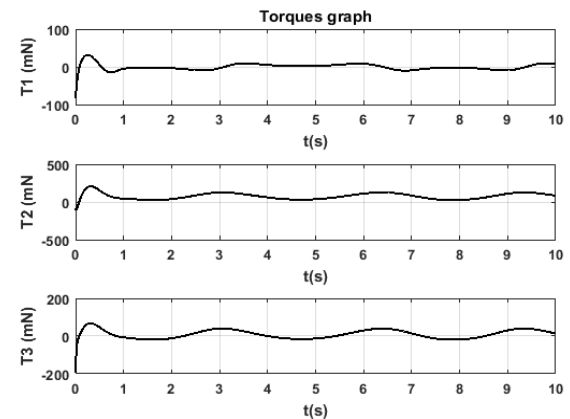Figure 16 shows the controls applied to achieve satisfactory convergence.

Figure 16 : Torques applied to motors.

7. CONCLUSION AND PERSPECTIVES

In this research work, we were interested in designing and manufacturing a small robot loader and unloader of a CNC machine tool. This manipulator will be used for practical

robotics works in our workshops. All mathematical models were developed and validated by simulations to justify the theoretical results found. Several Matlab scripts were developed and tested to make complex calculations and avoid possible errors.

The dynamic control proposed for the studied robot is very satisfactory; it suffices to act carefully on the various parameters that act on the regulation loop.

The realization part will be performed in collaboration with other departments. An infrastructure is already in place to finalize this work.

REFERENCES

1. Kantilal P.Rane, **Design and Development of Low Cost Humanoid Robot with Thermal Temperature Scanner for COVID-19 Virus Preliminary Identification,** *International Journal of Advanced Trends in Computer Science and Engineering*, Volume 9, No.3, pp. 3485 - 3493 , 2020.
2. Khalil W., Dombre E., **Modelisation, identification and control of robots,***HermesPenton Science*, London, ISBN 1-90399-613-9, 2002, 480.
3. Christoph Klug, Dieter Schmalstieg, Thomas Gloor, Clemens Arth, **A Complete Workflow for Automatic Forward Kinematics Model Extraction of Robotic Total Stations Using the Denavit-Hartenberg Convention,***Journal of Intelligent & Robotic Systems 95*, pp. 311–329, 2019. https://doi.org/10.1007/s10846-018-0931-4.
4. Ruthber Rodríguez Serrezuela, Adrián Fernando Chávarro Chavarro, Miguel Angel Tovar Cardozo1,Alejandro Leiva Toquica and Luis Fernando Ortiz Martinez, **Kinematic Modelling Of A Robotic Arm Manipulator Using Matlab,***ARPN Journal of Engineering and Applied Sciences,* VOL.12, NO. 7,pp.2037-2039, 2017.
5. Samia M. Mahil, Student Member, IEEE, Ahmed Al-Durra, Senior Member, IEEE, **ModelingAnalysis and Simulation of 2-DOF Robotic Manipulator,***2016 IEEE 59th International Midwest Symposium on Circuits and Systems (MWSCAS)*, pp. 16-19, 2016.
6. Yeyson Becerra, Mario Arbulu, Sebastian Soto, and Fernando Martinez, **A Comparison Among the Denavit-Hartenberg, the Screw Theory, and the Iterative Methods to Solve Inverse Kinematics for Assistant Robot Arm,***Springer Nature Switzerland AG 2019,*pp.447–457, 2019.https://doi.org/10.1007/978-3-030-26369-0_42.
7. Ramish, Syed Baqar Hussai, Farah Kanwa, **Design of a 3 DoF Robotic Arm,***The sixth international conference on Innovative Computing Technology(INTECH),* 2016,DOI: 10.1109/INTECH.2016.7845007.
8. Amin A. Mohammed and M. Sunar, **Kinematics Modeling of a 4-DOF Robotic Arm,** *International Conference on Control, Automation and Robotics, 2015,***DOI:** 10.1109/ICCAR.2015.7166008.
9. Amogh Patwardhan, Aditya Prakash, Rajeevlochana G. Chittawadigi, **Kinematic Analysis and Development of Simulation Softwarefor Nex Dexter Robotic Manipulator,***ScienceDirect, Procedia Computer Science,* Vol. 133, pp.660–667, 2018.
10. Aleksander K. Kovalchuk, Faniya Kh. Akhmetova, **Denavit-Hartenberg Coordinate System for Robotswith Tree-like Kinematic Structure,** *International Journal of Robotics and Automation (IJRA),*Vol. 5, No. 4, pp. 244-254, 2016.
11. Christoph Klug, Dieter Schmalstieg, Thomas Gloor & Clemens Arth, **A Complete Workflow for Automatic Forward Kinematics Model Extraction of Robotic Total Stations Using the Denavit-Hartenberg Convention,***Journal of Intelligent & Robotic Systems,* Vol. 95, pp. 311-329, 2019.
12. My El houssine ECH-CHHIBAT, Laidi ZAHIRI, Laila AIT EL MAALEM, **Modeling and simulation of a loader and unloader manipulator,***IEEE Conference on Innovative Research in Applied Science, Engineering and Technology (IRASET),* Meknes, Morocco, 16-19 April 2020.
13. Alaa Hassan, Mouhammad Abomoharam,**Modeling and design optimization of a robot gripper mechanism,** *Robotics and Computer--Integrated Manufacturing,* Vol. 46, pp. 94–103,2017.
14. Jorge Angeles, **Fundamentals of Robotic Mechanical Systems,** *Published by Springer International Publishing Switzerland 2014.*
15. Tomi J. Ylikorpi, Aarne J. Halme, Pekka J. Forsman,**Dynamic modeling and obstacle-crossing capability of flexiblependulum-driven ball-shaped robots,***Robotics and Autonomous Systems,* Vol. 87, pp. 269–280, 2017.
16. Mohsen Malayjerdi, Alireza Akbarzadeh, **Analytical modeling of a 3-D snake robot based on sidewindinglocomotion,***International Journal of Dynamics and Control,*pp. 83-93, 2019.
17. Dan B. Marghitu, **Mechanisms and RobotsAnalysis with MATLAB,** *Published bySpringer Dordrecht Heidelberg London New York, Springer-Verlag London Limited 2009.*
18. Peter Corke, **Robotics,Vision and Control,***Published by Springer International Publishing AG 2017.*
19. Supriyono, Wahyu Widiyanto, Waluyo Adi Siswanto, **Alternative Control System for Robot Arm with Data Logger,***International Journal of Advanced Trends in Computer Science and Engineering,* Volume 9, No.3, pp. 3728-3733 , 2020.
20. Syed Khalid Mustafa, MykhailoKopot, M. Ayaz Ahmad, Valentin Lyubchenko, VyacheslavLyashenko, **Interesting Applications of Mobile Robotic Motion by using Control Algorithms,** *International Journal of Advanced Trends in Computer Science and Engineering,* Volume 9, No.3, pp. 3847-3852.